

Src64 is required for ovarian ring canal morphogenesis during *Drosophila* oogenesis

G. Steven Dodson¹, Douglas J. Guarnieri^{1,2} and Michael A. Simon^{1,*}

¹Department of Biological Sciences and ²Department of Genetics, Stanford University, Stanford, CA 94305, USA

*Author for correspondence (e-mail: msimon@leland.stanford.edu)

Accepted 18 May; published on WWW 9 July 1998

SUMMARY

The Src family of protein tyrosine kinases have been implicated as important regulators of cellular proliferation, differentiation and function. In order to understand further the role of Src family kinases, we have generated loss-of-function mutations in *Src64*, one of two Src family kinases known in *Drosophila melanogaster*. Animals with reduced *Src64* function develop normally and are fully viable. However, *Src64* female flies have reduced fertility, which is associated with the incomplete transfer of cytoplasm from nurse cells to the developing oocyte. Analysis of *Src64* egg chambers showed defects in the ring canals that interconnect the oocyte and its 15 associated

nurse cells. *Src64* ring canals fail to accumulate the high levels of tyrosine phosphorylation that are normally present. Despite the reduced tyrosine phosphorylation, known ring canal components such as filamentous actin, a ring canal-specific product of the *hu-li tai shao* gene, and the *kelch* protein localize properly. However, *Src64* ring canals are reduced in size and frequently degenerate. These results indicate that *Src64* is required for the proper growth and stability of the ovarian ring canals.

Key words: Protein tyrosine kinase, src, *Src64*; Ring canal, *Drosophila*; Cytoskeleton, Egg chamber, Oogenesis

INTRODUCTION

The Src family of protein tyrosine kinases were first identified as transforming proteins encoded by oncogenic retroviruses (Collett and Erikson, 1978; Levinson et al., 1978). At present, nine distinct Src family kinases (SFKs) have been identified in vertebrates. The SFKs share a common domain structure consisting of an amino-terminal myristylation site, SH3 and SH2 domains, the protein tyrosine kinase catalytic domain and a carboxy-terminal regulatory region. Several of the vertebrate SFKs are expressed in specific hematopoietic lineages where their participation in receptor-mediated signaling is required for proper development and cellular function (for reviews of SFKs see Superti-Furga and Courtneidge, 1995; Brown and Cooper, 1996; Lowell and Soriano, 1996). The more broadly expressed SFKs (Src, Fyn and Yes) are activated in response to growth factors (such as PDGF, EGF, CSF-1) that signal through the activation of receptor tyrosine kinases (RTKs) (Ralston and Bishop, 1985; Osheroov and Levitzki, 1994; Courtneidge et al., 1993). Consistent with a role in RTK signaling, the inhibition of SFK function blocks mitogenesis in response to these growth factors (Twamley-Stein et al., 1993; Roche et al., 1995b). In addition to their involvement in receptor-mediated signaling, the inhibition of SFK function blocks the G₂-M transition of the cell cycle in fibroblasts (Roche et al., 1995a).

Numerous studies suggest that SFKs also function to regulate the actin cytoskeleton. Transformation of fibroblasts

with activated SFKs causes disruptions in the actin cytoskeleton (Boschek et al., 1981). These changes are associated with increased tyrosine phosphorylation of many cytoskeletal associated proteins. These include proteins involved in cell substrate adhesion (tensin, vinculin, talin, paxillin, FAK, β 1 integrin, p130^{cas}, AFAP110), cell-cell adhesion (plakoglobin, β -catenin, p120^{cas}) and other proteins thought to regulate the actin cytoskeleton (p190 rhoGAP and cortactin) (Brown and Cooper, 1996). SFK participation in cytoskeletal regulation is also supported by studies of *src*-deficient mice. These mice suffer from osteopetrosis, a bone remodeling disorder caused by a failure of osteoclast function (Soriano et al., 1991; Lowe et al., 1993). Examination of the *src*⁻ osteoclasts shows that they are deficient in the formation of ruffled borders and have defects in the underlying actin cytoskeleton (Boyce et al., 1992; Schwartzberg et al., 1997). Studies of fibroblasts derived from mice lacking Csk, a negative regulator of SFKs, have provided additional evidence for SFK involvement in actin cytoskeleton regulation. These cells have disrupted actin cytoskeletons and increased phosphorylation of p120, FAK, paxillin, tensin and cortactin. Furthermore, the removal of *src* activity suppresses the cytoskeletal defects of *csk*⁻ cells and returns the phosphorylation of tensin and cortactin to normal levels (Thomas et al., 1995).

The developing egg chamber of *Drosophila* is useful for the study of cytoskeletal regulation. In *Drosophila*, oogenesis proceeds through fourteen discrete stages prior to the

fertilization of the egg. (for a review of *Drosophila* oogenesis see Spradling, 1993). At the initiation of oogenesis, a single germline-derived cystoblast cell undergoes four rounds of mitotic divisions characterized by incomplete cytokinesis. As a result of the incomplete cytokinesis, these 16 germline cells are interconnected by a network of 15 cytoplasmic bridges called ring canals. One of the cells containing four ring canals becomes the developing oocyte while the 15 remaining cells differentiate as nurse cells. Surrounding each cluster of 16 cells is a sheath of somatically derived follicle cells. Early in oogenesis, the developing oocyte becomes transcriptionally inactive. Thus, most of the maternal products required for early embryogenesis are synthesized in the nurse cells and transported to the oocyte through the ring canals. Throughout most of oogenesis, the cytoplasmic transport from the nurse cells to the oocyte is gradual. At late stages (beginning at stage 11) of oogenesis, the nurse cells contract and rapidly transfer the remainder of their cytoplasmic contents to the oocyte (for a review on cytoplasmic transfer see Mahajan-Miklos and Cooley, 1994b). Following the completion of cytoplasmic transfer, the nurse cells degenerate.

The actin cytoskeletal rearrangements that occur during ring canal morphogenesis have been extensively studied (for a review of ring canals see Cooley and Robinson, 1996). Shortly after the arrest of the cleavage furrow, one or more unidentified phosphotyrosine-containing proteins localizes to the outer rim of the presumptive ring canal (Robinson et al., 1994). After the final mitotic divisions give rise to the 16 germ-cell cluster an inner rim forms at the ring canals. Initially, F-actin, a ring-canal-specific product (HTS-RC) of the *hu-li tai shao* (*hts*) gene and additional phosphotyrosine-containing protein(s) become localized to the inner rim of the ring canal (Robinson et al., 1994). The accumulation of F-actin is dependent on *hts* function since, in *hts* mutant egg chambers, the inner rim does not form at the majority of cytoplasmic bridges and only phosphotyrosine can be detected at most ring canals (Yue and Spradling, 1992; Robinson et al., 1994). Subsequent to the addition of F-actin, HTS-RC and phosphotyrosine protein(s), the *kelch* protein (Kelch) also becomes localized to the inner rim of the ring canal (Xue and Cooley, 1993). The function of Kelch is to maintain the compaction of the ring canal rim. In late stage *kelch* mutant egg chambers, F-actin diffuses into the inner lumen of the ring canals and partially blocks the transfer of nurse cell cytoplasm to the oocyte (Robinson et al., 1994; Tilney et al., 1996). In addition to these known components of the ring canal, the product of the *cheerio* gene is also required for proper ring canal formation. *cheerio* ring canals are small and lack F-actin, HTS-RC and Kelch. Furthermore, fusions between the nurse cell and the oocyte are frequently observed in *cheerio* egg chambers indicating that the integrity of the plasma membrane has been compromised (Robinson et al., 1997). The *cheerio* gene has not been cloned so it is not known whether its product is a ring canal component.

Once the ring canals are established, they do not remain static. The rims of newly formed ring canals have diameters of 0.5–1 μm (Warn et al., 1985). By stage 11, at the onset of rapid cytoplasmic transfer from the nurse cells to the oocyte, the ring canals have attained their maximum size with a diameter of roughly 10 μm . EM studies have shown that the early phase of growth (prior to stage 5) is accompanied by the addition of new actin filaments to the ring canal. After stage 5, there is an

increase in total F-actin at the ring canal, but it is unclear as to whether this increase results from the addition of new filaments or the lengthening of existing filaments. However, during this developmental period, the filaments become organized into large bundles (Tilney et al., 1996).

We have generated mutations in *Src64*, one of two known *Drosophila* SFKs, and shown that *Src64* function is required during ring canal morphogenesis. *Src64* mutant egg chambers have dramatically decreased levels of phosphotyrosine at their ring canals. F-actin, HTS-RC and Kelch each localize properly to *Src64* mutant ring canals despite the reduction of phosphotyrosine levels. However, *Src64* ring canals fail to grow as large as wild-type ring canals. Furthermore, the mutant ring canals often degenerate prior to the onset of rapid cytoplasmic transfer. As a consequence, the cytoplasmic transfer from nurse cells to the oocyte is incomplete resulting in small eggs and reduced female fertility. Based on these observations, we propose that SRC64 is a key regulator of the growth and stability of the ring canals.

MATERIALS AND METHODS

Drosophila stocks

All fly stocks were maintained under standard culture conditions. *w¹¹¹⁸* was used as wild type in these experiments. The BGT-T063 enhancer trap line, *w¹¹¹⁸; P[lwB]64C1-2*, was provided by Matthew Freeman and Gerry Rubin (University of California, Berkeley). The deficiency stock used in this study was *w¹¹¹⁸; Df(3L)10H/TM3, Sb*. For mobilization of the BGT-T063 P-element *w¹¹¹⁸; Ki, p^P, P[ry⁺, Delta2-3]* flies were used as a transposase source.

Characterization of the *Src64* transcription unit

The structure of the *Src64* transcription unit and the insertion site of the BGT-T063 P-element is based on direct nucleotide sequence comparison between genomic DNA and *Src64* cDNAs. Sequence of the genomic region containing the *Src64* protein-coding sequences was obtained by double-strand sequencing using directed primers based on the *Src64* cDNA sequence. Templates for the 5' non-coding region of the *Src64* were obtained by sonication of a BGT-T063 rescue plasmid and insertion of the sonicated fragments into the vector M13mp10. Plasmid rescue of genomic DNA flanking P-element insertions has been described previously (Wilson et al., 1989). All sequencing was done by the dideoxy chain termination method (Sanger et al., 1977) using a Sequenase kit (US Biochemicals). The third exon (28 bp) is present in the *Src64* cDNA and is unaccounted for in the genomic sequences from either the coding region or the 5' region of *Src64*. It is presumed to lie in the large region that separates the 5' end of the gene from the coding sequences.

Generation and molecular characterization of *Src64* alleles

The *Src64^{Δ17}* and *Src64^{Δ19}* alleles were isolated as imprecise excisions (Daniels et al., 1985) of the BGT-T063 P-element based on the loss of the *white* marker gene. DNA from 90 viable excision lines was used as templates for PCR reactions using the primers 5'-TAC-ACCGTTGAACGACTCGGACGCA-3' and 5'-GCGTTGGTCTC-CGAGGGGAAAGGC-3'. Genomic Southern analysis showed that the deletions in *Src64^{Δ17}* and *Src64^{Δ19}* do not extend beyond the *Cla*I restriction site 5' of the gene. The extent of the deletions into the gene has not been determined, but they remove most or all of the first two exons. Prior to the isolation of the *Src64^{PI}* allele, EMS mutagenesis was used to generate lines in which the *white* gene in the BGT-T063 P-element insertion was mutated and gave a light yellow rather than a dark red eye color. One of these lines was then used to identify

potential local transpositions based on a darker red eye due to the presence of more than one P-element insert. Among these potential local transpositions, the *Src64^{PI}* allele was identified due to its failure to complement the cytoplasmic transfer defect of the *Src64^{Δ17}* allele. The structure of *Src64^{PI}* was determined by restriction digests and Southern blot analysis of rescue plasmids from the P-element insertions. The cytoplasmic transfer defect of *Src64^{PI}* is revertible at high frequency (19/68). Genomic Southern analysis on *Src64^{PI}* revertant lines indicates that mutant phenotypes are associated with the downstream P-element inserted within the *Src64* transcription unit. For all the *Src64* alleles, the cytoplasmic transfer defects are more severe when the alleles are *in trans* to a deficiency for *Src64*. For example, 55% of *Src64^{PI}* stage 14 egg chambers show a clear cytoplasmic transfer defect, while 80% of *Src64^{PI}/Df3L(10H)* stage 14 egg chambers are defective. These results suggest that none of the alleles are fully null for *Src64* function.

Fertility analysis

An equal number of 2- to 5-day-old mutant or wild-type virgin females were crossed to wild-type males and their eggs collected on a molasses agar plate and counted at 24 hour intervals. The eggs were allowed to develop for another 28-30 hours and then examined under a dissecting microscope to quantitate the hatched versus unhatched eggs. These experiments were conducted at 25°C.

Generation of the anti-SRC64 serum

A rat anti-Src64 serum was generated to a GST-SRC64 fusion protein. A 4.2 kb *NcoI-HindIII* genomic DNA fragment was cloned into the pGEX-KG vector. The protein was expressed and purified from *E. coli* with glutathione affinity chromatography as previously described (Smith and Johnson, 1988) and injected into rats. The GST-SRC64 fusion protein contains the first 88 amino acids of the *Src64* protein plus six random amino acids from the fourth intron of the *Src64* gene.

Immunocytochemistry and imaging

Ovaries from 2- to 5-day-old females maintained in yeasted vials in the presence of wild-type male flies were dissected in phosphate-buffered saline (PBS). Fixation and antibody staining have been described previously (Cooley et al., 1992; Robinson et al., 1994). The anti-SRC64 serum was used at a 1:500 dilution. The HTS-RC and Kelch hybridoma supernatant were used at 1:1 dilution. The anti-phosphotyrosine antibody PY20 (Transduction Laboratories) was used at a 1:1000 dilution. For staining egg chambers with propidium iodide and fluorescein phalloidin, fixed egg chambers were treated with 400 μg/ml RNase A in phosphate-buffered saline (PBS) for 2 hours at room temperature. Egg chambers were then rinsed three times in PBS and incubated in a 10 μg/ml solution of propidium iodide (Molecular Probes) in PBS for 20 minutes on a rocking platform. Egg chambers were then rinsed 3× 5 minutes in PBS and incubated in a solution of fluorescein phalloidin in PBS (Molecular Probes) (5 μl of fluorescein phalloidin vacuum dried and resuspended 100 μl of PBS) for 20 minutes on a rocking platform in the dark. For triple staining, fixed egg chambers were first treated with RNase A, then incubated with antibodies. Following the antibody incubation and rinses, the egg chambers were stained with propidium iodide and fluorescein phalloidin as described above. All egg chambers were mounted in citifluor glycerol (Ted Pella). Images of the egg chambers were taken on a MRC 1024 confocal laser microscope (BioRad) using the CoMOS software. Images of eggs in Fig. 3C,D were taken on a Zeiss Axiophot microscope using dark field optics. The images of egg chambers in Fig. 3A,B were taken using DIC optics.

Ring canal measurements

Ring canal measurements were taken of HTS-RC-stained ring canals. The images were enlarged, printed on a dye sublimation printer and measured by hand. Only the outer diameter of the ring canals was measured. Staging of egg chambers was according to Spradling

(1993). Stage 5 egg chambers were identified based on their size (55×75 μm). Stage 10A egg chambers were identified based on the initiation of centripetal follicle cell migration and the absence of the actin halo that forms at stage 10B. For each stage, the average size of the ring canals from individual egg chambers was determined. These averages were then averaged to give the reported ring canal sizes.

Immunoblots

Protein extracts from a 0-16 hour embryo collection and ovaries were prepared by directly homogenizing the tissues in Laemmli buffer. Proteins were separated on a SDS-PAGE gel and transferred to nitrocellulose membranes. The membranes were blocked by incubation in Tris-buffered saline+0.5% Tween 20 (TBST)+5% w/v of dry milk. The blots were then incubated with the anti-SRC64 serum at a 1:1000 dilution in TBST+5% dry milk overnight at 4°C. Blots were rinsed in TBST 4× 15 minutes prior to incubation with a peroxidase-coupled secondary antibody. The protein was detected using the ECL detection kit (Amersham).

Germline transformation

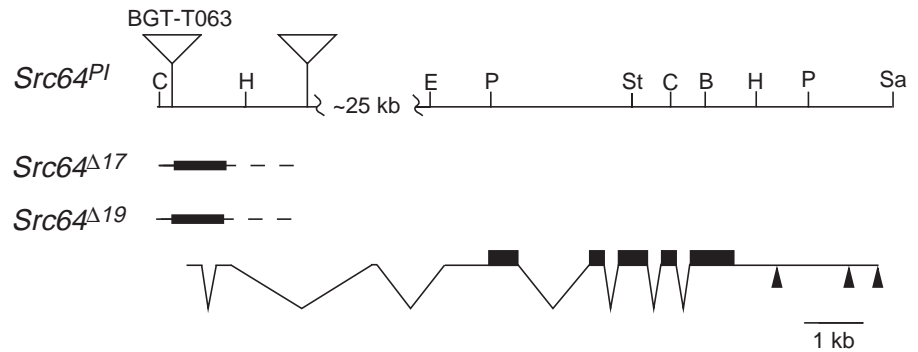
A 7 kb *ApaI-SalI* genomic fragment of *Src64*, containing the *Src64* protein-coding sequences, was cloned into the D277Matg vector provided by Daniel St Johnston. This vector is identical to the modified pCaTub67CMatpolyA vector described previously (Micklem et al., 1997), except that the initiation ATG of *Tub67c* has been mutated to ATT. The cloning produced a transcriptional fusion between *Tub67c* and the untranslated region in the fourth exon of *Src64* approximately 300 bp upstream of the *Src64* initiation ATG.

RESULTS

We began our efforts to identify *Src64* mutations by analyzing an enhancer trap line, BGT-T063, in which a P-element containing the *white* and *lacZ* genes was inserted near *Src64* in the 64C1 polytene band of the third chromosome. Flies that are homozygous for the BGT-T063 P-element are viable and fertile. In order to map the location of the P-element insertion relative to the *Src64* locus, we obtained genomic DNA flanking the P-element insertion site by plasmid rescue. Analysis of this DNA indicated that the P-element was inserted approximately 50 base pairs upstream of the 5' end of our longest *Src64* cDNA (Fig. 1). Despite the proximity of the BGT-T063 P-element to the *Src64* transcription unit, homozygous BGT-T063 embryos still express significant levels of *Src64* protein (data not shown). However, flies in which the BGT-T063 P-element is placed *in trans* to a deficiency for the *Src64* locus do occasionally show the mutant phenotypes described below thus indicating that the BGT-T063 insertion probably generates a very weak *Src64* allele.

In order to identify strong *Src64* mutations, we took advantage of the fact that transposase catalyzed P-element excision frequently results in the deletion of flanking DNA sequences. 200 lines of flies were established that contained chromosomes from which the BGT-T063 P-element had excised. Eight of the 200 excision chromosomes carried recessive lethal mutations. These eight lethal mutations either failed to map to the *Src64* region or affected a previously identified gene near *Src64* (data not shown). Since none of the homozygous lethal excisions appeared to affect *Src64*, we screened the homozygous viable excision chromosomes for lesions affecting the *Src64* transcription unit. PCR primers were designed to amplify a 545 bp fragment from the non-

Fig. 1. Molecular structure of *Src64* alleles. A restriction map of the *Src64* genomic region with the cDNA structure shown below (C, *Cla*I; H, *Hind*III; E, *Eco*RI; P, *Pst*I; B, *Bam*HI; St, *Stu*I; Sa, *Sal*I). The protein-coding exons are indicated by the black boxes and approximate polyadenylation sites by arrow heads. Exon three in the untranslated 5' region cDNA has not been mapped precisely to the genomic DNA. The *Src64^{PI}* allele is an insertion of a P-element generated by local transposition of the BGT-T063 P-element. Both the original BGT-T063 P-element and a second element inserted approximately 2.5 kb downstream in the second intron are present in the *Src64^{PI}* allele. The *Src64^{Δ17}* and *Src64^{Δ19}* alleles are deletions generated by imprecise excision of the BGT-T063 P-element. Each deletion, shown as black boxes below the transcription unit, removes most or all of the first two non-coding exons. Neither deletion extends beyond the *Cla*I site 5' of the gene.



coding first and second exons of the *Src64* locus. Genomic DNA from two lines, *Src64^{Δ17}* and *Src64^{Δ19}*, failed to yield PCR products suggesting that each of these excisions removed at least one of the PCR priming sites. Southern analysis confirmed that both excisions had deleted most or all of the first two exons of *Src64* (Fig. 1). An additional *Src64* allele was subsequently generated by local transposition of the BGT-T063 P-element. This allele, *Src64^{PI}*, is also homozygous viable and fails to complement *Src64^{Δ17}* with respect to the cytoplasmic transfer phenotype described below. Analysis of the *Src64^{PI}* allele indicated that a second P-element was inserted in the second intron approximately 2.5 kb downstream of the BGT-T063 element (Fig. 1). Since each of the *Src64* alleles affected only non-coding sequences, we examined their effects on SRC64 expression in ovaries and 0-16 hour embryos. This analysis indicated that SRC64 expression is greatly reduced by the *Src64^{PI}* and *Src64^{Δ17}* mutations (Fig. 2). However, neither allele entirely eliminates SRC64 production.

***Src64* mutations disrupt cytoplasmic transfer during oogenesis**

Each of the *Src64* alleles is viable both *in trans* to each other and to a deficiency for the *Src64* region. However, females homozygous for any of the three alleles have reduced fertility (Table 1). Eggs laid by *Src64* females hatch at reduced frequency when compared to wild type. In addition, *Src64* females lay fewer eggs than wild type, which may suggest that the defective eggs are resorbed as has been previously observed for other female-sterile mutations (Spradling, 1993). In contrast, *Src64* males are fully fertile. The loss of female fertility is associated with a defect in cytoplasmic transfer from the nurse cells to the developing oocyte. Unlike wild-type egg chambers, 55% of late stage *Src64* egg chambers have nurse cell cytoplasm remaining at the anterior end of the oocyte (Fig. 3A,B). As a result, eggs from *Src64* females range from 50%-100% of the length of eggs oviposited by wild-type females (Fig. 3C,D). Both the reduction of female fertility and the defect in cytoplasmic transfer can be reverted by excision of the downstream P-element present in the *Src64^{PI}* allele (data not shown). This indicates that these phenotypes are due to disruption of the *Src64* gene.

***Src64* mutations alter ring canal morphogenesis**

Incomplete cytoplasmic transfer is often indicative of defects in the actin cytoskeleton of the nurse cells. Two unique cytoskeletal features are particularly important for efficient transfer. The first is the formation prior to the rapid transfer phase (stage 10B) of actin cables that hold the nurse cell nuclei in place. In the absence of these actin cables, the nurse cell nuclei become lodged in the ring canals and block transfer (Cooley et al., 1992; Cant et al., 1994; Mahajan-Miklos and Cooley, 1994a; Guild et al., 1997). Staining of *Src64* egg chambers with fluorescein-conjugated phalloidin to visualize filamentous actin at stage 10B showed that the actin cables were present (data not shown). The second important cytoskeletal structure of the nurse cells are the ring canals. In order to assess the role of SRC64 in ring canal morphogenesis,

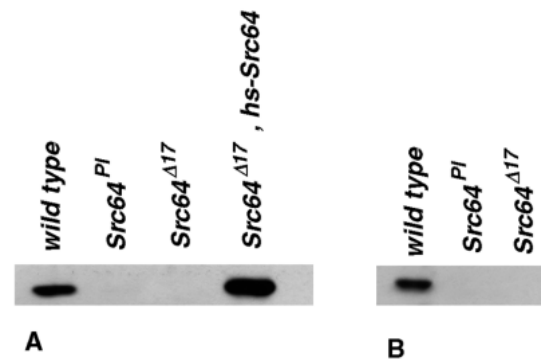


Fig. 2. Immunoblots on 0-16 hour embryonic (A) and ovarian (B) protein extracts using anti-SRC64 serum. The genotypes of the animals from which the extracts were derived are indicated above each lane. The *hs-Src64*, *Src64^{Δ17}* extract is from *Src64^{Δ17}* embryos in which a wild-type *Src64* was expressed under the control of the *Hsp70* promoter. The presence of immunoreactive protein in this lane confirms that the 62 kDa protein shown is the product of *Src64*. A low level of SRC64 could be detected in the mutant extracts when the blot was overexposed indicating that the mutations do not completely abolish SRC64 expression. Amido Black staining of the membranes following immunodetection showed that total protein loaded in each lane was equivalent.

Table 1. *Src64* mutant females have reduced fertility

Female genotype	Eggs laid/fly/hour	Hatch rate
wild type	0.94	94.7% (n=321)
<i>Src64^{PI}</i>	0.11	5.5% (n=291)
<i>Src64^{Δ17}</i>	0.18	20.0% (n=454)
<i>Src64^{Δ19}</i>	0.68	37.9% (n=145)

Shown are the number of eggs oviposited and the hatch rates for eggs oviposited by females of the indicated genotype when crossed to wild-type males.

early to mid-stage mutant egg chambers were stained with fluorescein phalloidin and with antibodies directed against phosphotyrosine, HTS-RC or Kelch. These experiments showed that the normal complement of 15 ring canals was present and that F-actin, HTS-RC and Kelch all localize properly at the ring canals (Fig. 4A-F). The intensity of the staining for these components did not differ appreciably from that observed for wild-type ring canals, but the ring canal morphology appeared abnormal (discussed below). In contrast, there was a significantly reduced level of anti-phosphotyrosine staining in *Src64* egg chambers (Fig. 4G,H). This reduction was particularly dramatic at the ring canals, where only faint staining could generally be observed. However, mutant ring canals that maintained elevated anti-phosphotyrosine were observed occasionally. Reduced anti-phosphotyrosine staining was also observed in the cortical regions of the mutant nurse cells. These results indicate that *Src64* function is required for the majority of phosphotyrosine accumulation at ring canals, but that the formation of the ring canals and the localization of known ring canal components does not depend on this accumulation.

During our analysis of ring canal morphogenesis, we observed that *Src64* ring canals were smaller than their wild-

type counterparts. This phenotype was particularly obvious in the later stages of oogenesis (Fig. 5A,B). This effect was quantitated by measuring the outer ring canal diameters during both mid and late stages (stages 5 and 10A) of oogenesis. In stage 5 wild-type egg chambers, the ring canals vary in size between 2.0 and 4.5 μm with an average size of 3.1 μm . In contrast, *Src64^{PI}* ring canals vary in size from 1.0-3.5 μm with an average size 2.6 μm (Fig. 5D). The difference in ring canal size is more apparent at stage 10A (Fig. 5E). At this stage, wild-type ring canals vary between 6 and 14 μm with an average diameter of 9.5 μm . This represents a 3.1-fold increase in the average outer diameter of wild-type ring canals between stage 5 and stage 10A. In *Src64^{PI}* egg chambers, there is only a 2.3-fold increase in ring canal diameter between stages 5 and 10A. *Src64^{PI}* ring canals range from 3-10 μm with an average of 5.9 μm . These measurements indicate that ring canal growth is defective during both early and late phases of ring canal morphogenesis. In order to assess whether these smaller ring canals had other morphological abnormalities, F-actin-, HTS-RC- and Kelch-stained ring canals were examined at high magnification (Fig. 5C). The small ring canals appeared normal except for the presence of a slightly concave inner rim that is reminiscent of the inner rims of earlier stage wild-type ring canals.

We also observed that many (45%) stage 10A *Src64^{PI}* egg chambers contained fewer than 15 ring canals. *Src64^{Δ17}* and *Src64^{Δ19}* egg chambers also showed this phenotype but to a lesser extent. This reduction in ring canal number was only observed in stage 9-10 egg chambers, indicating that some ring canals must degenerate during these later stages of oogenesis. One possible consequence of ring canal degeneration would be fusion between cells. Evidence for such fusions was sought by staining mutant egg chambers with fluorescein phalloidin to visualize the filamentous cortical actin at the nurse cell boundaries, and propidium iodide to visualize the nurse cell nuclei. At stages 9-10 approximately 70% of *Src64^{PI}* mutant

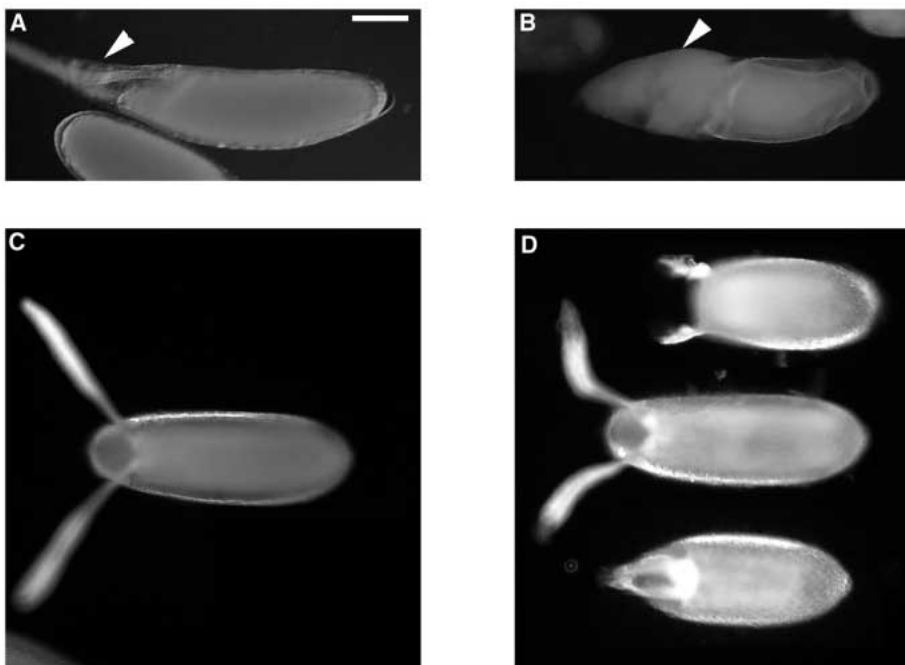


Fig. 3. Stage 14 egg chambers and eggs from wild-type and *Src64^{PI}* females. (A) Stage 14 egg chamber (lateral view) from a wild-type female. The arrowhead points to the region of the developing egg where the nurse cells have transferred their cytoplasm and degenerated. (B) Stage 14 egg chamber (lateral view) from a *Src64^{PI}* female. The arrowhead points to the remnants of the nurse cells that have failed to transfer their cytoplasm and degenerate. The amount of nurse cell cytoplasm that remains associated with the developing egg is variable for all the alleles we have generated. (C) Egg oviposited by a wild-type female (dorsal view). The structures that extend out from each egg are dorsal appendages, chorionic structures required for embryonic gas exchange. (D) Eggs oviposited by *Src64^{PI}* females. The egg size is variable and can range from 50%-100% the length of wild-type eggs. The eggs shown range from 70%-100% the length of a wild-type egg. The scale bar for A-D is 100 μm . Anterior is shown to the left.

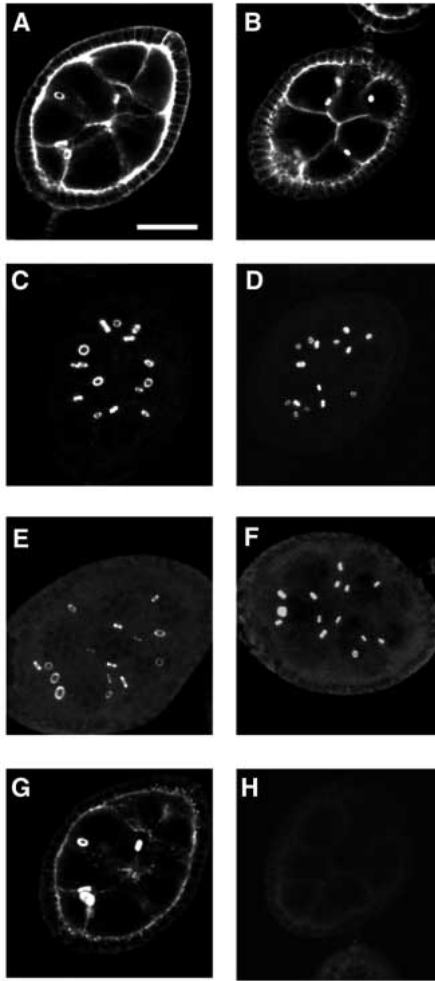


Fig. 4. Mid-stage egg chambers (stages 5-7) from wild-type and *Src64^{PI}* females. (A) Wild-type egg chamber stained with fluorescein phalloidin to visualize filamentous actin. (B) *Src64^{PI}* egg chamber stained with fluorescein phalloidin. (C) Wild-type egg chamber stained for HTS-RC. (D) *Src64^{PI}* egg chamber stained for HTS-RC. (E) Wild-type egg chamber stained for Kelch. (F) *Src64^{PI}* egg chamber stained for Kelch. (G) Wild-type egg chamber stained for phosphotyrosine. (H) *Src64^{PI}* egg chamber stained for phosphotyrosine. The scale bar for A-H is 25 μm . A, B, G, H are single optical sections through the egg chambers. In C-F, a series of optical sections through the egg chambers have been merged into a single image.

egg chambers had fusions between nurse cells (Fig. 6B). Nurse cell fusion was also observed in *Src64^{AI7}* egg chambers at a lower frequency (Fig. 6C). In only one case did we observe a fusion between the nurse cells and the oocyte. Interestingly, in rare cases, we observed cytoplasmic F-actin-containing structures that appeared to be ring canals that had detached from the cortical actin. To show that these structures were ring canals, we stained the mutant egg chambers with fluorescein phalloidin, propidium iodide and anti-Kelch antibodies. This experiment confirmed that the structures within the cytoplasm contain ring canal components (Fig. 6D,E). The morphology of the detached ring canals was often aberrant. Their F-actin appeared more diffuse than normal which suggests that they may have been in the process of degeneration. These

observations suggest that SRC64 is required to maintain the association between the ring canal and either the cortical actin or plasma membrane. Loss of attachment may lead to ring canal degeneration and nurse cell fusion.

SRC64 is enriched at ring canals

The altered morphogenesis and stability of *Src64* ring canals and their reduced phosphotyrosine content suggested that SRC64 might be a ring canal component. To test this possibility, wild-type egg chambers were stained with anti-SRC64 antibodies. Specific staining was detected in the cortex of the nurse cells and appeared enriched at the ring canals in wild type, but not *Src64^{AI7}*, egg chambers (Fig. 7A-D). Co-staining for F-actin and SRC64 showed that SRC64 localization overlaps F-actin at the ring canal (Fig. 7E). These results are consistent with SRC64 being localized to the nurse cell and oocyte plasma membranes as well as at the inner rim of the ring canals.

Ring canal defects can be rescued by germline expression of *Src64*

As a final confirmation that the phenotypes that we observed are due to *Src64* mutations, we rescued the *Src64* defects by expression of wild-type SRC64 in the germline of *Src64^{PI}* mutant females. A female germline-specific expression vector in which transcription is driven from the *Tub67C* promoter was used (Micklem et al., 1997; Matthews et al., 1989). The entire *Src64*-coding region was inserted into this vector and then introduced into the *Drosophila* genome by P-element-mediated germline transformation. We found that expression of *Src64* in *Src64^{PI}* egg chambers (Fig. 8C-D) partially rescued the ring canal growth defects. At stage 10A, the rescued ring canals averaged 8.5 μm in diameter, which is slightly smaller than in wild type (9.5 μm) but significantly larger than in the mutant (5.9 μm). Consistent with this rescue, elevated levels of anti-phosphotyrosine immunostaining were restored to the ring canals (Fig. 8A,B). Furthermore, the hatch rate of the eggs laid by *Src64^{PI}* females carrying the *Tub67c:Src64* transgene was increased from 5.5 to 68% and the rescued females laid morphologically normal eggs. These results confirm that the mutant phenotypes are due to the lack of *Src64* function.

DISCUSSION

We have generated mutations in the *Src64* gene by both imprecise excision and local transposition of a nearby P-element. Analysis of animals homozygous for either of the strongest two alleles indicates that *Src64* protein expression is severely reduced. Despite reduced SRC64 expression, these flies are viable. Their only observable phenotype is partial loss of female fertility that is associated with an inability to completely transfer cytoplasm from nurse cells to the developing oocyte. Previous studies have shown that this cytoplasmic transfer is critically dependent on the integrity of the ring canals that interconnect the oocyte with its nurse cells. We therefore investigated the role of SRC64 during ring canal morphogenesis.

The most apparent defect in *Src64* ring canals is their failure to grow at normal rates and to achieve wild-type size. The reduced size at stage 5 demonstrates that SRC64 function is

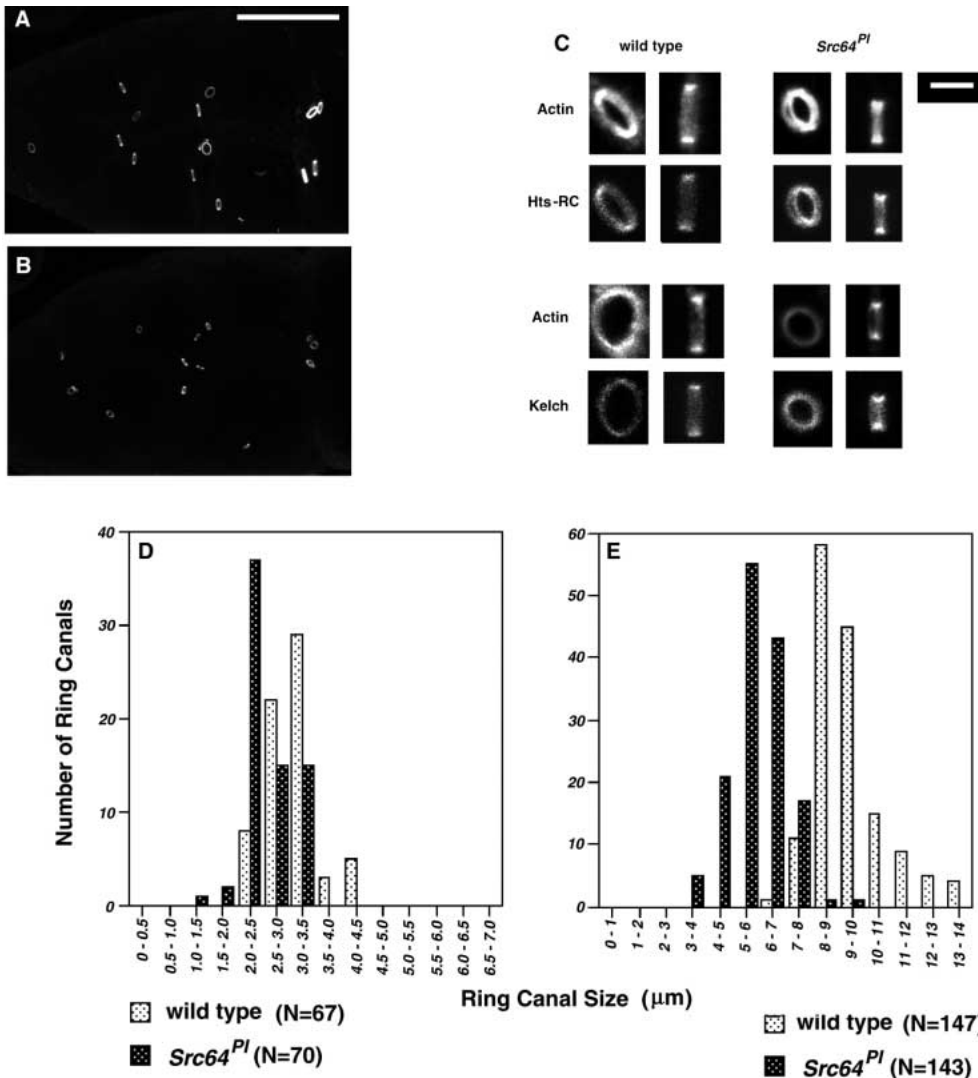


Fig. 5. Growth of ovarian ring canals is defective in *Src64* egg chambers. (A) Wild-type stage 10A egg chamber stained for HTS-RC. (B) *Src64^{PI}* stage 10A egg chamber stained for HTS-RC. Both A and B are a series of optical sections merged into one image. The scale bar for A-B is 50 μm. Anterior is to the left. (C) Individual wild-type and *Src64^{PI}* early stage 10A ring canals stained for F-actin, HTS-RC and Kelch. The scale bar is 5 μm (D) Ring canal size distribution of wild-type (white bars) and *Src64^{PI}* (black bars) stage 5 egg chambers. The average ring canal size of wild-type egg chambers at stage 5 is 3.1 μm with a standard deviation of 0.2. The average ring canal size of *Src64^{PI}* egg chambers at stage 5 is 2.6 μm with a standard deviation of 0.3. (E) Ring canal size distribution of wild type (white bars) and *Src64^{PI}* (black bars) for stage 10A egg chambers. The average ring canal size of wild-type egg chambers at stage 10A is 9.5 μm with a standard deviation of 0.7. The average ring canal size of *Src64^{PI}* egg chambers at stage 10A is 5.9 μm with a standard deviation of 0.8. For C and D, the outer diameter of HTS-RC-stained ring canals was measured. The differences in ring canal sizes between wild type and *Src64^{PI}* are significant ($P < 0.05$ for a Student's *t*-test) at both stages.

required during the early phase of ring canal growth. Our measurements at stage 10A indicate that *Src64* ring canals also grow slowly during the late phase of ring canal morphogenesis. In addition, the association between the ring canals and the plasma membrane/cortical actin is compromised during the later stages of oogenesis. These results suggest that SRC64 function may be required throughout ring canal development. However, we cannot exclude the possibility that the critical period for SRC64 function is early and that the failure of SRC64 to act early indirectly affects the late phase growth and stability of the ring canals.

Among the earliest detectable markers of developing ring canals is phosphotyrosine. The accumulation of phosphotyrosine-containing proteins is followed by the recruitment to the ring canals of F-actin and ring-canal-specific proteins such as HTS-RC and Kelch. We find that phosphotyrosine epitopes fail to accumulate in most *Src64* ring canals. This indicates that the majority of tyrosine phosphorylation of ring canal proteins is in response to SRC64 function. Despite the low level of phosphotyrosine at *Src64* ring canals, F-actin, HTS-RC and Kelch all localize properly. This suggests that the phosphorylation of components of the

arrested cleavage furrow is not essential for the recruitment of any of the known ring canal components. Instead, the slow growth of *Src64* ring canals and their observed detachment from the plasma membrane are consistent with a role for SRC64 in regulating reorganization of the ring canal rim and its attachment to the plasma membrane during ring canal growth.

SRC64 localization to the ring canals has important implications for the role of SRC64-dependent phosphorylation at the ring canal. One possibility is that SRC64 directly phosphorylates structural components of the ring canal in order to regulate ring canal morphogenesis. Alternatively, SRC64 may activate other protein tyrosine kinases that then phosphorylate inner rim components. The study of vertebrate SFKs has provided evidence for the activation of other protein tyrosine kinases by SFKs. For example, the transformation of cells by the activated *v-src* protein leads to the tyrosine phosphorylation and activation of focal adhesion kinase (FAK) (Kanner et al., 1990; Schaller et al., 1992; Guan and Shalloway, 1992). Studies have demonstrated a crucial role for FAK in regulating the actin cytoskeleton during cell-substratum adhesion (Illc et al., 1995). Vertebrate studies have also shown

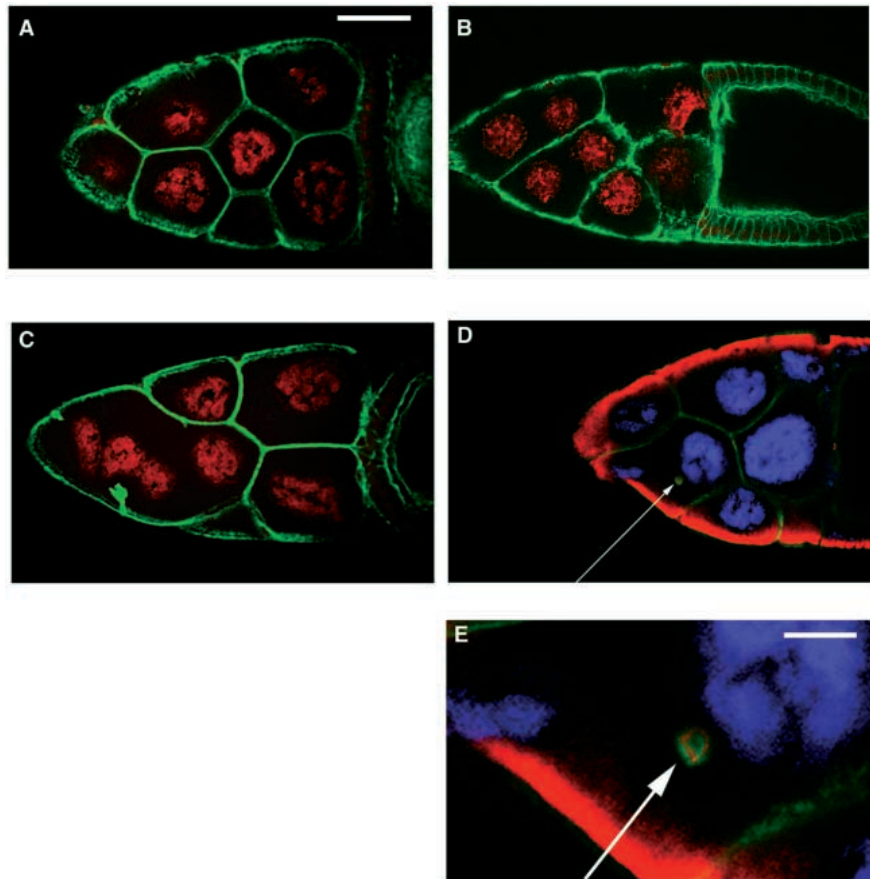


Fig. 6. Nurse cell fusion and ring canal degeneration in *Src64* mutant egg chambers. (A–C) Stage 10 egg chambers stained with fluorescein phalloidin (shown in green) to visualize the nurse cell boundaries and propidium iodide (shown in red) to visualize the nurse cell nuclei. (A) Wild-type egg chamber; (B) *Src64^{PI}* egg chamber; (C) *Src64^{Δ17}* egg chamber. Nurse cell fusions in B and C are visible as cells with more than one nuclei surrounded by cortical actin. (D) *Src64^{Δ17}* egg chamber triple labeled with propidium iodide (shown in purple) fluorescein phalloidin (shown in green) and antibodies against Kelch (shown in red). The arrow indicates a detached ring canal within the cytoplasm of the fused nurse cells. The red cortical staining is non-specific background occasionally observed when working with the anti-Kelch antibodies (E) An enlargement of the detached ring canal in D. The scale bar in A is 50 μm . The scale bar in E is 12.5 μm . Anterior is to the left.

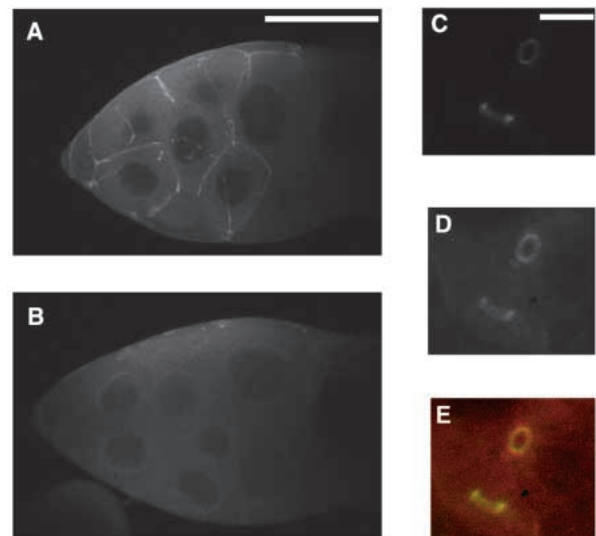
that members of the Tec family of tyrosine kinases, such as Bruton's Tyrosine Kinase (BTK), can be activated by SFKs (Mahajan et al., 1995; Rawlings et al., 1996; Afar et al., 1996). Interestingly, we and others have recently shown that a *Drosophila* Tec family kinase, TEC29, is both localized to the ring canal in a SRC64-dependent manner and is required for proper ring canal growth (Guarnieri et al., 1998; Roulier et al., 1998).

Does *Src64* have other functions during *Drosophila* development?

Previous studies have suggested that SRC64 may function at other times during *Drosophila* development. *Src64* mRNA is broadly expressed throughout development with elevated

levels detectable in the central nervous system (CNS) and developing visceral mesoderm of embryos and early pupae. High levels of *Src64* were also detected in the photoreceptors of third instar eye imaginal discs (Simon et al., 1985). Since no *Src64* alleles were available prior to this report, previous attempts to examine the role of SRC64 have relied on ectopic expression of a kinase inactive *Src64* protein. In some cases, kinase inactive forms of SFKs have been shown to mimic the effects of disrupting the corresponding gene (Cooke et al.,

Fig. 7. SRC64 localization in egg chambers. (A) Wild-type stage 10 egg chamber stained with an antibody directed against the N-terminal domain of SRC64. SRC64 is detectable at the cortex of the nurse cells. In other sections, SRC64 can also be detected at the cortex of the oocyte. SRC64 was detected as early as stage 2. Prior to stage 2 the high background staining of the antibodies prevented unambiguous detection of the protein. (B) A *Src64^{Δ17}* stage 10 egg chamber stained with the anti-SRC64 antibodies. (C) Wild-type ring canals from an early stage egg chamber stained with fluorescein phalloidin to visualize the filamentous actin. (D) The same ring canals as in C stained with the anti-SRC64 antibodies. (E) A merged image of C and D with F-actin shown in green and Src64 in red. The resulting yellow ring canals indicate that SRC64 colocalizes with actin at the ring canal. The scale bar for A and B is 100 μm . The scale bar for C and D is 10 μm .



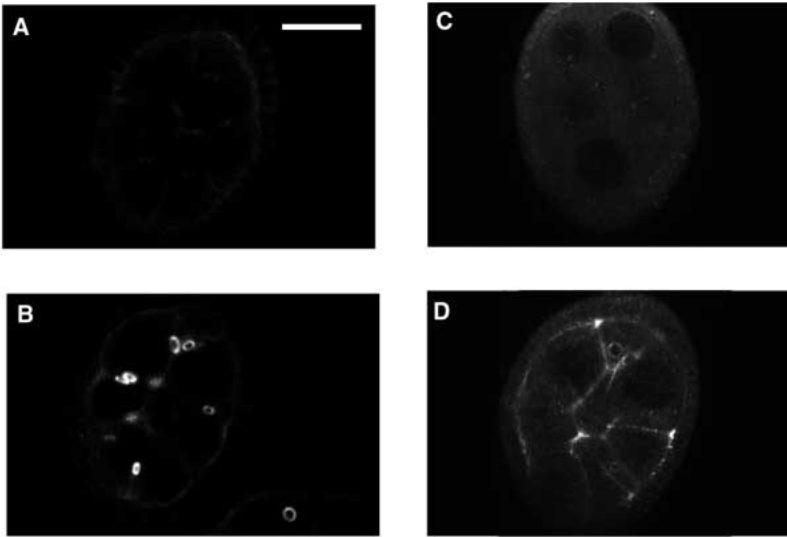


Fig. 8. Expression of wild-type *Src64* in the female germline increases phosphotyrosine levels at *Src64* ring canals. (A) *Src64^{PI}* mutant egg chamber stained with an antibody directed against phosphotyrosine. (B) A *Src64^{PI}* mutant egg chamber that carries one copy of the wild-type *Src64* gene expressed from the *Tub67c* promoter stained for phosphotyrosine. (C) A *Src64^{PI}* mutant egg chamber stained for SRC64. (D) A *Src64^{PI}* egg chamber that carries one copy of the wild-type *Src64* gene expressed from the *Tub67c* promoter stained for SRC64. The scale bar is 25 μ m.

1991; Stein et al., 1992; Appleby et al., 1992; Levin et al., 1993; Molina et al., 1992). In the case of SRC64, ubiquitous overexpression of the kinase inactive protein during embryogenesis led to defects in CNS development. During eye development, expression under *sevenless* transcriptional control of the kinase inactive SRC64 led to the loss of photoreceptors (Kussick et al., 1993). These results suggested that SRC64 might have an important role in CNS and photoreceptor development. However, we have been unable to detect any CNS or photoreceptor defects in *Src64* animals. One possible explanation for this discrepancy is that the amount of SRC64 required during CNS and photoreceptor development is much lower than that required during oogenesis. Thus, the very low level of SRC64 present in the mutant animals might be sufficient for these processes. Alternatively, expression of the kinase inactive SRC64 may interfere with biochemical pathways in which SRC64 either does not normally participate or in which SRC64 function can be replaced by SRC41, the second *Drosophila* SFK (Takahashi et al., 1996).

The idea that some cellular functions can be performed by more than one SFK has been supported by previous studies. For example, while mice lacking either *hck* or *fgf* do not display any significant defects in myeloid development or function, the neutrophils of *hck⁻fgf⁻* mice show severe defects in certain integrin-mediated cellular responses (Lowell et al., 1994; Lowell et al., 1996a). Similarly, while the osteoclasts of *hck⁻* mice function normally, the removal of *hck* from *src⁻* mice markedly increases the severity of the *src⁻* osteoclast defect (Lowell et al., 1996b). In fibroblasts, inhibition of Src alone during G₂ of the cell cycle does not have any dramatic effect on cell cycle progression. However, inhibition of Src, Fyn and Yes causes an arrest of the cell cycle at the G₂-M transition (Roche et al., 1995a).

During embryonic and larval development, the expression of *Src41* largely overlaps *Src64* including high levels of expression in the CNS and visceral mesoderm (Takahashi et al., 1996). Thus SRC41 may be able to compensate for a lack of SRC64 in these tissues. Interestingly, the lack of maternally contributed *Src41* in preblastoderm embryos suggests that the female germline is a tissue where SRC41 expression may not overlap that of SRC64. This difference in expression patterns may explain why the *Src64*

mutant phenotype is limited to defects in oogenesis. Ultimately, understanding the full range of SRC64 and SFK function during *Drosophila* development will require the identification of mutations in *Src41* and any as yet unidentified *Drosophila* SFKs.

We thank Dr Matthew Freeman for his initial isolation of the BGT-T063 P-element, Dr Daniel St. Johnston for the germline expression vector and Carrie Steinberg for the injection of P-element constructs. We would like to thank members of our laboratory for their many helpful comments on this manuscript and work. We would also like to thank Dr Lynn Cooley and members of her laboratory, especially D. Robinson, for helpful discussions and the generous donation of antibodies. The early stages of this work were performed in the laboratories of Drs J. Michael Bishop and Gerald M. Rubin. This study was supported by a grant from the National Eye Institute (1R01EY9845) and an NSF National Young Investigator Award (MCB-9357009). During the course of this work, M. A. S. was a Searle Scholar, a Lucille P. Markey Scholar in Biomedical Sciences, and a Terman Fellow. G. S. D. and D. J. G. were supported by an NIH predoctoral training grant.

REFERENCES

- Afar, D. E., Park, H., Howell, B. W., Rawlings, D. J., Cooper, J. and Witte, O. N. (1996). Regulation of Btk by Src family tyrosine kinases. *Mol. Cell Biol.* **16**, 3465-3471.
- Appleby, M. W., Gross, J. A., Cooke, M. P., Levin, S. D., Qian, X. and Perlmutter, R. M. (1992). Defective T cell receptor signaling in mice lacking the thymic isoform of p59fyn. *Cell* **70**, 751-763.
- Boschek, C. B., Jockusch, B. M., Friis, R. R., Back, R., Grundmann, E. and Bauer, H. (1981). Early changes in the distribution and organization of microfilament proteins during cell transformation. *Cell* **24**, 175-184.
- Boyce, B. F., Yoneda, T., Lowe, C., Soriano, P. and Mundy, G. R. (1992). Requirement of pp60c-src expression for osteoclasts to form ruffled borders and resorb bone in mice. *J. Clin. Invest.* **90**, 1622-1627.
- Brown, M. T. and Cooper, J. A. (1996). Regulation, substrates and functions of src. *Biochim. Biophys. Acta* **1287**, 121-149.
- Cant, K., Knowles, B. A., Mooseker, M. S. and Cooley, L. (1994). *Drosophila* singed, a fascin homolog, is required for actin bundle formation during oogenesis and bristle extension. *J. Cell Biol.* **125**, 369-380.
- Collett, M. S. and Erikson, R. L. (1978). Protein kinase activity associated with the avian sarcoma virus src gene product. *Proc. Natl. Acad. Sci. USA* **75**, 2021-2024.
- Cooke, M. P., Abraham, K. M., Forbush, K. A. and Perlmutter, R. M. (1991). Regulation of T cell receptor signaling by a src family protein-tyrosine kinase (p59fyn). *Cell* **65**, 281-291.
- Cooley, L., Verheyen, E. and Ayers, K. (1992). chickadee encodes a profilin

- required for intercellular cytoplasm transport during *Drosophila* oogenesis. *Cell* **69**, 173-184.
- Cooley, L. and Robinson, D. N.** (1996). Stable intercellular bridges in development: the cytoskeleton lining the tunnel. *Trends Cell Biol.* **6**, 474-479.
- Courtneidge, S. A., Dhand, R., Pilat, D., Twamley, G. M., Waterfield, M. D. and Roussel, M. F.** (1993). Activation of Src family kinases by colony stimulating factor-1, and their association with its receptor. *EMBO J.* **12**, 943-950.
- Daniels, S. B., McCarron, M., Love, C. and Chovnick, A.** (1985). Dysgenesis-induced instability of rosy locus transformation in *Drosophila melanogaster*: analysis of excision events and the selective recovery of control element deletions. *Genetics* **109**, 95-117.
- Guan, J. L. and Shalloway, D.** (1992). Regulation of focal adhesion-associated protein tyrosine kinase by both cellular adhesion and oncogenic transformation. *Nature* **358**, 690-692.
- Guarnieri, D. J., Dodson, G. S. and Simon, M. A.** (1998) Src64 regulates the localization of a Tec family kinase for *Drosophila* ring canal growth. *Mol. Cell* **1**, 831-840.
- Guild, G. M., Conelly, P. S., Shaw, M. K. and Tilney, L. G.** (1997). Actin filament cables in *Drosophila* nurse cells are composed of modules that slide passively past one another during dumping. *J. Cell Biol.* **134**, 783-797.
- Ille, D., Furuta, Y., Kanazawa, S., Takeda, N., Sobue, K., Nakatsuji, N., Nomura, S., Fujimoto, J., Okada, M. and Yamamoto, T.** (1995). Reduced cell motility and enhanced focal adhesion contact formation in cells from FAK-deficient mice. *Nature* **377**, 539-544.
- Kanner, S. B., Reynolds, A. B., Vines, R. R. and Parsons, J. T.** (1990). Monoclonal antibodies to individual tyrosine-phosphorylated protein substrates of oncogene-encoded tyrosine kinases. *Proc. Natl. Acad. Sci. U. S. A.* **87**, 3328-3332.
- Kussick, S. J., Basler, K. and Cooper, J. A.** (1993). Ras1-dependent signaling by ectopically-expressed *Drosophila* src gene product in the embryo and developing eye. *Oncogene* **8**, 2791-2803.
- Levin, S. D., Anderson, S. J., Forbush, K. A. and Perlmutter, R. M.** (1993). A dominant-negative transgene defines a role for p56lck in thymopoiesis. *EMBO J.* **12**, 1671-1680.
- Levinson, A. D., Oppermann, H., Levintow, L., Varmus, H. E. and Bishop, J. M.** (1978). Evidence that the transforming gene of avian sarcoma virus encodes a protein kinase associated with a phosphoprotein. *Cell* **15**, 561-572.
- Lowe, C., Yoneda, T., Boyce, B. F., Chen, H., Mundy, G. R. and Soriano, P.** (1993). Osteopetrosis in Src-deficient mice is due to an autonomous defect of osteoclasts. *Proc. Natl. Acad. Sci. USA* **90**, 4485-4489.
- Lowell, C. A., Soriano, P. and Varmus, H. E.** (1994). Functional overlap in the src gene family: inactivation of hck and fgr impairs natural immunity. *Genes Dev.* **8**, 387-398.
- Lowell, C. A., Fumagalli, L. and Berton, G.** (1996a). Deficiency of Src family kinases p59/61hck and p58c-fgr results in defective adhesion-dependent neutrophil functions. *J. Cell Biol.* **133**, 895-910.
- Lowell, C. A., Niwa, M., Soriano, P. and Varmus, H. E.** (1996b). Deficiency of the Hck and Src tyrosine kinases results in extreme levels of extramedullary hematopoiesis. *Blood* **87**, 1780-1792.
- Lowell, C. A. and Soriano, P.** (1996c). Knockouts of Src-family kinases: stiff bones, wimpy T cells, and bad memories. *Genes Dev.* **10**, 1845-1857.
- Mahajan, S., Fargnoli, J., Burkhardt, A. L., Kut, S. A., Saouaf, S. J. and Bolen, J. B.** (1995). Src family protein tyrosine kinases induce autoactivation of Bruton's tyrosine kinase. *Mol. Cell Biol.* **15**, 5304-5311.
- Mahajan-Miklos, S. and Cooley, L.** (1994a). The villin-like protein encoded by the *Drosophila* quail gene is required for actin bundle assembly during oogenesis. *Cell* **78**, 291-301.
- Mahajan-Miklos, S. and Cooley, L.** (1994b). Intercellular cytoplasm transport during *Drosophila* oogenesis. *Dev. Biol.* **165**, 336-351.
- Matthews, K. A., Miller, D. F. and Kaufman, T. C.** (1989). Developmental distribution of RNA and protein products of the *Drosophila* alpha-tubulin gene family. *Dev Biol.* **132**, 45-61.
- Micklem, D. R., Dasgupta, R., Elliott, H., Gergely, F., Davidson, C., Brand, A., Gonzalez-Reyes, A. and St.Johnston, D.** (1997). The mago nashi gene is required for the polarisation of the oocyte and the formation of perpendicular axes in *Drosophila*. *Curr. Biol.* **7**, 468-478.
- Molina, T. J., Kishihara, K., Siderovski, D. P., van Ewijk, W., Narendran, A., Timms, E., Wakeham, A., Paige, C. J., Hartmann, K. U. and Veillette, A.** (1992). Profound block in thymocyte development in mice lacking p56lck. *Nature* **357**, 161-164.
- Osherov, N. and Levitzki, A.** (1994). Epidermal-growth-factor-dependent activation of the src-family kinases. *Eur. J. Biochem.* **225**, 1047-1053.
- Ralston, R. and Bishop, J. M.** (1985). The product of the protooncogene c-src is modified during the cellular response to platelet-derived growth factor. *Proc. Natl. Acad. Sci. USA* **82**, 7845-7849.
- Rawlings, D. J., Scharenberg, A. M., Park, H., Wahl, M. I., Lin, S., Kato, R. M., Fluckiger, A. C., Witte, O. N. and Kinet, J. P.** (1996). Activation of BTK by a phosphorylation mechanism initiated by SRC family kinases. *Science* **271**, 822-825.
- Robinson, D. N., Cant, K. and Cooley, L.** (1994). Morphogenesis of *Drosophila* ovarian ring canals. *Development* **120**, 2015-2025.
- Robinson, D. N., Smith-Leiker, T. A., Sokol, N. S., Hudson, A. M. and Cooley, L.** (1997). Formation of the *Drosophila* ovarian ring canal inner rim depends on cheerio. *Genetics* **145**, 1063-1072.
- Roche, S., Fumagalli, S. and Courtneidge, S. A.** (1995a). Requirement for Src family protein tyrosine kinases in G2 for fibroblast cell division. *Science* **269**, 1567-1569.
- Roche, S., Koegl, M., Barone, M. V., Roussel, M. F. and Courtneidge, S. A.** (1995b). DNA synthesis induced by some but not all growth factors requires Src family protein tyrosine kinases. *Mol. Cell Biol.* **15**, 1102-1109.
- Roulier, E. M., Panzer, S. and Beckendorf, S. K.** (1998). The nonreceptor tyrosine kinase Tec29A is required during *Drosophila* embryogenesis and interacts with Src64B in ring canal development. *Mol. Cell* **1**, 819-829.
- Sanger, F., Nicklen, S. and Coulson, A. R.** (1977). DNA sequencing with chain-terminating inhibitors. *Proc. Natl. Acad. Sci. USA* **74**, 5463-5467.
- Schaller, M. D., Borgman, C. A., Cobb, B. S., Vines, R. R., Reynolds, A. B. and Parsons, J. T.** (1992). pp125FAK a structurally distinctive protein-tyrosine kinase associated with focal adhesions. *Proc. Natl. Acad. Sci. USA* **89**, 5192-5196.
- Schwartzberg, P. L., Xing, L., Hoffman, O., Lowell, C. A., Garrett, L., Boyce, B. F. and Varmus, H. E.** (1997). Rescue of osteoclast function by transgenic expression of kinase-deficient Src in src^{-/-} mutant mice. *Genes Dev.* **11**, 2835-2844.
- Simon, M. A., Drees, B., Kornberg, T. and Bishop, J. M.** (1985). The nucleotide sequence and the tissue-specific expression of *Drosophila* c-src. *Cell* **42**, 831-840.
- Smith, D. B. and Johnson, K. S.** (1988). Single-step purification of polypeptides expressed in *Escherichia coli* as fusions with glutathione S-transferase. *Gene* **67**, 31-40.
- Soriano, P., Montgomery, C., Geske, R. and Bradley, A.** (1991). Targeted disruption of the c-src proto-oncogene leads to osteopetrosis in mice. *Cell* **64**, 693-702.
- Spradling, A. C.** (1993). Developmental Genetics of Oogenesis. In *The Development of Drosophila melanogaster* (ed. M. Bate and A. Martinez Arias), pp. 1-70. Plainview, NY: Cold Spring Harbor Laboratory Press.
- Stein, P. L., Lee, H. M., Rich, S. and Soriano, P.** (1992). pp59fyn mutant mice display differential signaling in thymocytes and peripheral T cells. *Cell* **70**, 741-750.
- Superti-Furga, G. and Courtneidge, S. A.** (1995). Structure-function relationships in Src family and related protein tyrosine kinases. *BioEssays* **17**, 321-330.
- Takahashi, F., Endo, S., Kojima, T. and Saigo, K.** (1996). Regulation of cell-cell contacts in developing *Drosophila* eyes by Dsrc41, a new, close relative of vertebrate c-src. *Genes Dev.* **10**, 1645-1656.
- Thomas, S. M., Soriano, P. and Imamoto, A.** (1995). Specific and redundant roles of Src and Fyn in organizing the cytoskeleton. *Nature* **376**, 267-271.
- Tilney, L. G., Tilney, M. S. and Guild, G. M.** (1996). Formation of actin filament bundles in the ring canals of developing *Drosophila* follicles. *J. Cell Biol.* **133**, 61-74.
- Twamley-Stein, G. M., Pepperkok, R., Anson, W. and Courtneidge, S. A.** (1993). The Src family tyrosine kinases are required for platelet-derived growth factor-mediated signal transduction in NIH 3T3 cells. *Proc. Natl. Acad. Sci. USA* **90**, 7696-7700.
- Warn, R. M., Gutzeit, H. O., Smith, L. and Warn, A.** (1985). F-actin rings are associated with the ring canals of the *Drosophila* egg chamber. *Exp. Cell Res.* **157**, 355-363.
- Wilson, C., Pearson, R. K., Bellen, H. J., O'Kane, C. J., Grossniklaus, U. and Gehring, W. J.** (1989). P-element-mediated enhancer detection: an efficient method for isolating and characterizing developmentally regulated genes in *Drosophila*. *Genes Dev.* **3**, 1301-1313.
- Xue, F. and Cooley, L.** (1993). kelch encodes a component of intercellular bridges in *Drosophila* egg chambers. *Cell* **72**, 681-693.
- Yue, L. and Spradling, A. C.** (1992). hu-li tai shao, a gene required for ring canal formation during *Drosophila* oogenesis, encodes a homolog of adducin. *Genes Dev.* **6**, 2443-2454.